

# Development of First-Order Gradiometer-type MI Sensor and its Application for a Metallic Contaminant Detection System

T. Takiya, T. Uchiyama, and H. Aoyama\*

Graduate School of Engineering, Nagoya Univ., Chikusa-ku, Nagoya, Aichi 464-8603, Japan

\*Aichi Steel Co., 1 Wano-Wari, Arao-machi, Tokai, Aichi 476-8666, Japan

A first-order gradiometer-type MI sensor that can reduce environmental magnetic noise without a magnetic shield was developed. The noise spectral density of this sensor is 20 pT/Hz<sup>1/2</sup> at 1–30 Hz, which is as good as a commercial fluxgate sensor, and the noise at 60 Hz relating to the power source line is reduced. We detected SUS304 austenitic stainless steel balls with the developed MI gradiometer to simulate a system for detecting metallic contaminants using the MI sensor. The variation of magnetic field with moving SUS304 balls corresponds to the theoretical value obtained for the model of a steel ball. This MI sensor without a magnetic shield system provides a compact and simple method of detecting metallic contaminants.

**Key words:** MI sensor, gradiometer, fluxgate magnetometer, metallic contaminant detection system

## 1. Introduction

High-sensitivity magnetometers are used in industry, for measurement of biomagnetism, and other applications. The magneto-impedance (MI) sensor can detect microscopic magnetic signals ranging from mT (10<sup>-3</sup> T) to pT (10<sup>-12</sup> T) by utilizing the magneto-impedance (MI) effect<sup>1)</sup>. In the MI effect, the impedance of an amorphous wire changes significantly when a high-frequency current is passed through the amorphous wire<sup>2)</sup>. A CMOS-MI sensor which can discriminate magnetic poles by measuring the voltage induced in a pick-up coil wound with amorphous wire was developed in 2002<sup>3)</sup>.

MI sensors have been studied for use in various fields<sup>4-6)</sup>; we are considering utilizing the MI sensor for non-destructive inspections. Recently, there have been various cases of contamination of food, and metal accounts for 14% of all such contamination according to a national survey in 2014<sup>7)</sup>. Metal detectors or X-ray examination are the most common methods of detecting foreign metal substances. As a more sensitive detection method, a Superconducting Quantum Interference Element (SQUID) sensing system, which can detect the magnetic field relating to the residual magnetization of metal, has been developed<sup>8)</sup>. The MI sensor also can detect metal substances using the measurement principle of SQUID, and a contaminant detection system with an MI sensor has been realized<sup>9)</sup>. The advantage of the MI sensing method is that it can detect metal without a magnetic shield system by using a gradiometer comprising a pair of MI sensors. The MI sensor is expected to provide a compact, low-price system for detecting metallic contaminants in food.

In this study, we developed a first-order gradiometer-type MI sensor (MI gradiometer) that can reduce the influence of external magnetic noise, and measured the variation of magnetic field with moving SUS304 balls to simulate a metallic contaminant

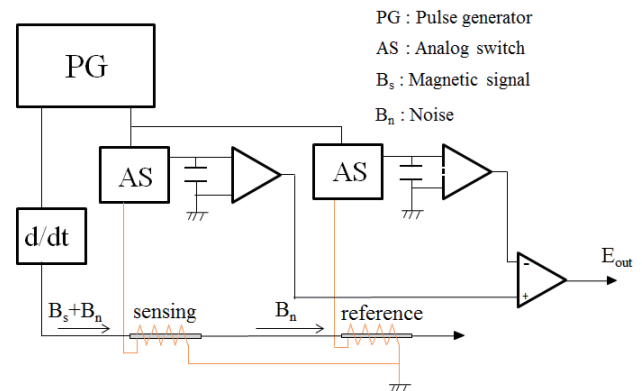


Fig. 1 First-order gradiometer type MI sensor.

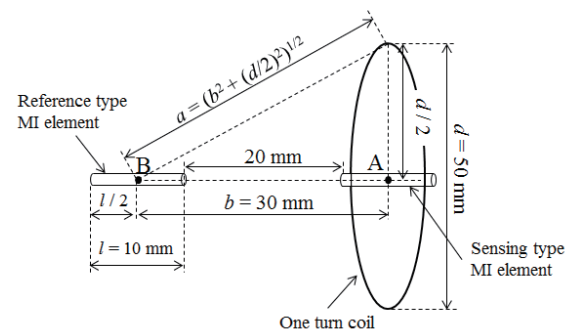
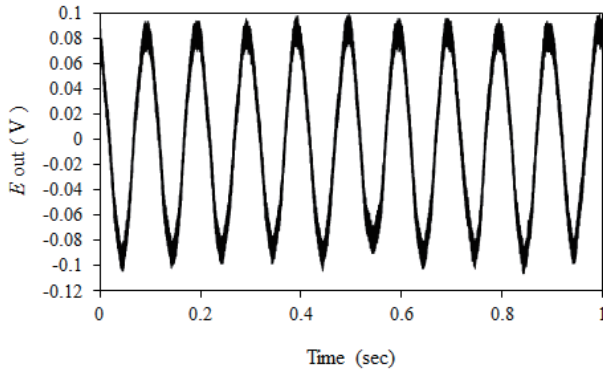


Fig. 2 Position of one-turn coil and MI elements.

detection system using the MI sensor.

## 2. First-order gradiometer-type MI sensor

The first-order gradiometer-type MI sensor (MI gradiometer) is composed of a pair of CMOS-MI sensors (Fig. 1). The high-frequency current is passed through a sensing-type and a reference-type MI element after the voltage is differentiated by a pulse generator (CMOS multi-vibrator). The MI gradiometer outputs the difference of the voltage induced in two pick-up coils: a wound sensing-type MI element and a reference-type MI



**Fig. 3** Output of MI gradiometer when a sine voltage is applied to a one-turn coil.

element.

The length of the sensor head is 50 mm. The amorphous wire (Aichi Steel Co., Ltd.) used in the sensor head is 25  $\mu\text{m}$  in diameter and 40 mm in length. The distance between the sensing and reference element is set at 20 mm from the center of both elements. The pick-up coils of each MI element have 700 turns. The frequency band of the MI gradiometer is 1–30 Hz. The magnetic sensitivity of the sensing MI element is  $46 \times 10^6$  V/T in a static magnetic field because the sensitivity is increased 1167 times with amplifiers. The magnetic sensitivity of the gradiometer is  $1.53 \times 10^9$  V/(T/m) when the magnetic sensitivity of the sensing element is divided by the distance (30 mm) between the sensing-type and reference-type MI elements.

We confirmed the operation of the developed MI gradiometer by detecting an artificial signal produced by a one-turn coil (diameter  $d = 50$  mm, impedance  $z = 20$  k $\Omega$ ). Figure 2 shows a one-turn coil to which is applied sine voltage  $v$  (amplitude: 2 V, frequency: 10 Hz) set in the center of the sensing-type MI element (point A). According to Biot-Savart's law, Eq. (1) and (2) represent the magnetic flux density at point A,  $B_A$ , and point B,  $B_B$ .

$$B_A = \mu_0 H_A = \mu_0 (i / d) \quad (1)$$

$$B_B = \mu_0 H_B = \mu_0 [i (d / 2)^2 / 2b^3] \quad (2)$$

where  $H_A$  is the magnetic field at point A,  $H_B$  is the magnetic field at point B,  $i = v/z$ ,  $d = 50$  mm,  $b = (b^2 + (d/2)^2)^{1/2}$ ,  $c = 30$  mm,  $l = 10$  mm, and  $\mu_0 = 4\pi \times 10^{-7}$ . Consequently,  $B_A$  is 2.51 nT and  $B_B$  is 0.662 nT.

The output of the MI gradiometer,  $E_{\text{out}}$ , is shown in Fig. 3. The average amplitude of  $E_{\text{out}}$  is 0.09 V and its frequency is 10 Hz. The detected magnetic signal of the MI gradiometer corresponds to 1.96 nT when  $E_{\text{out}}$  is divided by the magnetic sensitivity of the sensing-type MI element,  $46 \times 10^6$  V/T. This measured value approximates  $B_A - B_B = 1.85$  nT of the theoretical magnetic signal of the MI gradiometer. Therefore, the developed MI gradiometer operates correctly.

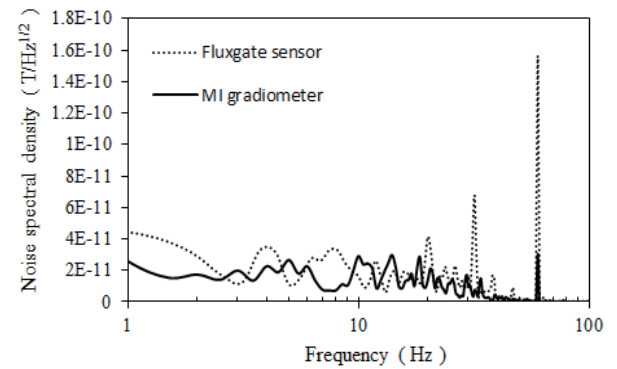


**Fig. 4** Comparison of external magnetic noise spectral density between MI gradiometer and fluxgate sensor.

### 3. Comparison with a fluxgate sensor

We measured the environmental magnetic noise spectral density in the laboratory with the MI gradiometer and a fluxgate sensor (Fluxmaster, Stefan Mayer Instruments). The magnetic sensitivity is  $46 \times 10^6$  V/T for the sensing-type MI element of the MI gradiometer and 10 V/ $\mu\text{T}$  for the fluxgate sensor in a static magnetic field, and both sensors are set to a cut-off frequency of 30 Hz with a multi-function filter (3611, NF Corporation).

The environmental noise spectral density is shown in Fig. 4. The magnetic noise at 1 Hz is 40 pT/Hz $^{1/2}$  in the fluxgate magnetometer and 20 pT/Hz $^{1/2}$  in the MI gradiometer. The noise at 60 Hz relating to the power source line reaches about 160 pT/Hz $^{1/2}$  in the fluxgate sensor, whereas that of the MI gradiometer is 30 pT/Hz $^{1/2}$  and the noise at 30 Hz also is reduced significantly. This result indicates that the MI gradiometer is robust against environmental magnetic noise.

### 4. Detection of SUS304 balls using MI sensor

Firstly, we detected SUS304 austenitic stainless steel balls with the MI gradiometer. Figure 5 is a photograph of a SUS304 ball which was used for the experiment and Table 1 lists the chemical composition of SUS304 according to the JIS standard. SUS304 is a corrosion-resistant stainless steel widely used in products ranging from household items to industrial goods. SUS304 is nonmagnetic austenite (face-centered-cubic structure) but when stress is applied the metal becomes magnetized due to the formation of martensite<sup>10)</sup>. Figure 6 shows the set-up for measuring the variation of magnetic field when the SUS304 ball was moved at various distances,  $r$ , from the sensor head to the steel ball. The SUS304 ball was placed on a turntable rotated at 7.5 m/min. The diameter of the SUS304 ball,  $d_s$ , was 0.15 mm, 0.3 mm, 0.5 mm, 0.8 mm, 1.0 mm and 1.5 mm.

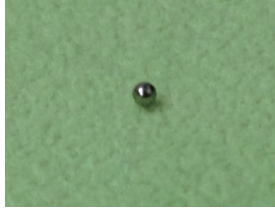


**Fig. 5** Stainless steel ball of SUS304 (1.0 mm diameter).

**Table 1** Chemical composition of SUS304

Element	C	Si	Mn	P	S	Ni	Cr
	≤	≤	≤	≤	≤	8.00	18.00
Mass%	0.08	1.00	2.00	0.045	0.030	~	~
						10.50	20.00

We compared the theoretical value of magnetic field of the model of the steel ball (Fig. 7) and the value measured with the MI gradiometer,  $\Delta B$ . The external magnetic field of the SUS304 ball,  $H$ , at point  $p$  is given by Eq. (3) which is obtained from Fig. 7<sup>11)</sup>.

$$B = \mu_0 H = \mu_0 (m / 2 \pi \mu_0 r^3) \cos \theta \quad (3)$$

Where  $d_s \ll r$ ,  $B$  is the magnetic flux density and  $m$  is the residual magnetic moment of SUS304.  $\theta$  is assumed to be  $0^\circ$  since SUS304 is magnetized in the longitudinal direction of an amorphous wire by using a permanent magnet. We measured  $m$  with a VSM. The residual magnetic field of the VSM was calibrated with a gauss meter and we postulated that  $m$  is the residual magnetic moment when the magnetic field of electromagnets is 0.

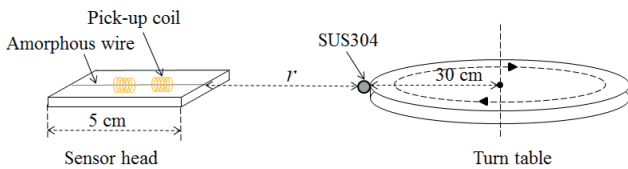


**Fig. 6** Measurement setup for SUS304.

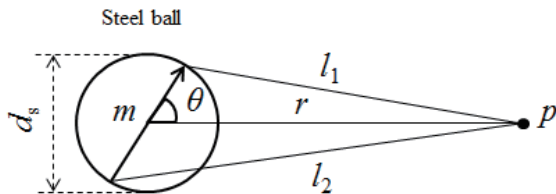


**Fig. 7** Model of steel ball.

Figure 8 shows the output voltage of the MI gradiometer,  $E_{out}$ , for the moving SUS304 ball of each diameter when  $r$  was 10 mm. The maximum  $E_{out}$  is 3.0 V at  $d_s = 1.5$  mm, and the minimum is 90 mV at  $d_s = 0.15$  mm. However,  $E_{out}$  is not proportional to  $d_s$  but is proportional to  $m$ . We consider that this phenomenon results from the difference in processing degree of each

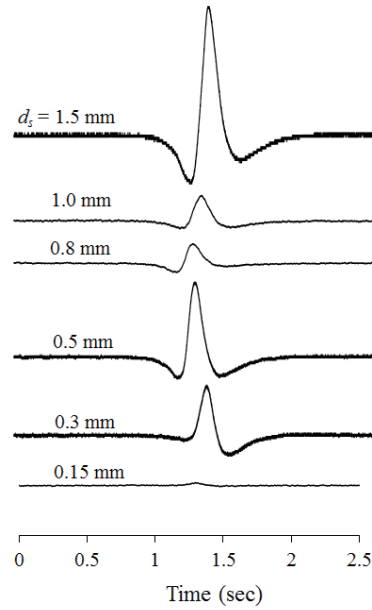


**Fig. 8** Output voltage of MI gradiometer with movement of SUS304 steel balls.

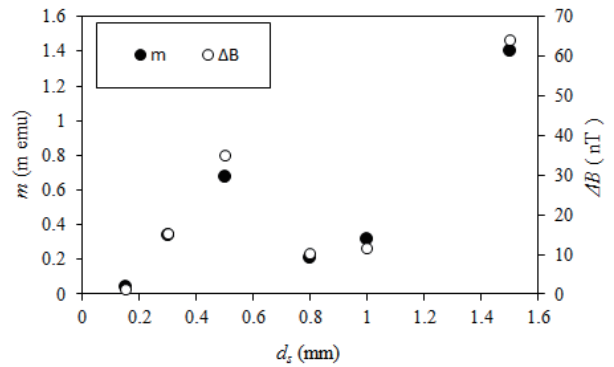


**Fig. 9** Relationship between residual magnetic moment,  $m$ , and value measured with MI gradiometer,  $\Delta B$ .

SUS304 ball.  $\Delta B$  is calculated by dividing  $E_{out}$  by  $46 \times 10^6$  V/T and Fig. 9 confirms that  $\Delta B$  is proportional to  $m$ .

Secondly, we examined the lowest limit of AC magnetic field of the MI gradiometer without a shield box made of permalloy. We estimate that the detection for SUS304 ball of 0.3 mm diameter is the benchmark of performance evaluation because the lowest detection limit of the X-ray detector is about 0.6–0.7 mm diameter<sup>12)</sup>. For this reason, the detection target of the MI gradiometer is an SUS304 ball of  $d_s = 0.3$  mm. In addition, we detected a SUS304 ball with the fluxgate sensor “Fluxmaster”. Since the maximum rotational velocity of the turntable which we used is 7.5 m/min, the cut-off frequency of both sensors was set at 30 Hz with the 3611 multi-function filter.

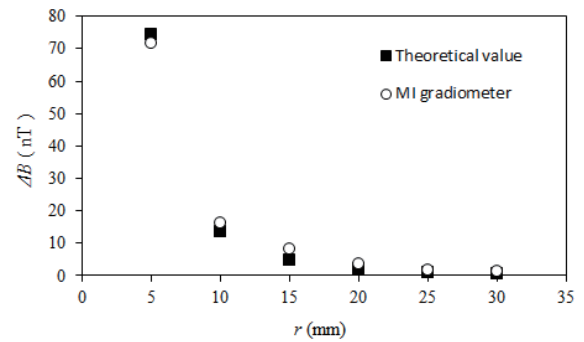
Figure 10 shows the dependence of the variation of the magnetic field with moving SUS304 ball and various distances between sensor head and SUS304 ball. Figure 10(a) compares  $\Delta B$  between the measured value and the theoretical value derived from Eq. (3). The measured

**Table 2** Comparison between existing contaminant detection system and MI sensor system.

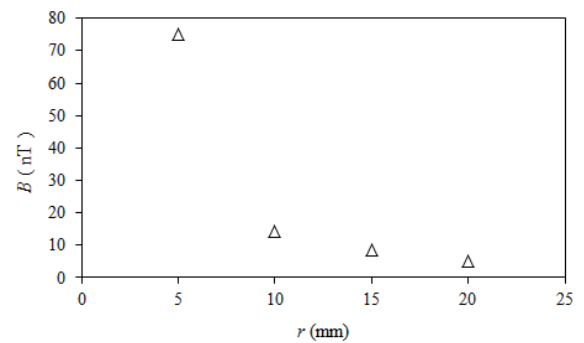
	Detection lowest limit	Unusable food	Detection without metal
Metal detector	Depends on conductivity of metal substance	No food	×
X-ray	$\phi$ 0.6–0.7 mm	Dairy products	○
MI sensor	$\phi$ 0.3 mm	No food	×

value is calculated by dividing  $E_{out}$  by the magnetic sensitivity of the sensing-type MI element ( $46 \times 10^6$  V/T). For example, when  $r$  was fixed at 5 mm, the theoretical value of  $B$  was calculated from Eq. (3) for each distance  $r$  from 5 mm to 14 mm because the length of a sensing-type MI element is 10 mm. The average  $B$  value was then calculated. Similarly, we calculated the average  $B$  value of a reference-type MI element. The theoretical value of  $\Delta B$  was taken as the difference between the average  $B$  values of the sensing and reference-type MI elements. The measured value of  $\Delta B$  corresponds with the theoretical value and the lowest  $\Delta B$  is 1.20 nT at  $r = 30$  mm in Fig. 10(a). Figure 10(b) shows the measurement result when using the fluxgate sensor. The lowest magnetic flux density is 5.28 nT at  $r = 20$  mm. Figure 11 shows the output of both sensors at  $r = 25$  mm. The MI gradiometer reduces the environmental magnetic noise compared with the fluxgate sensor and the detected signal is clear.

We considered a system for detecting contaminants using the MI gradiometer. We estimate that the smallest stainless steel ball with weak magnetism like SUS304 that can be detected is 0.3 mm in diameter assuming that several MI gradiometers are located at the top and bottom of the belt conveyor. For example, frozen food packages can pass between MI sensors in this case. Metal detectors and X-ray examination are the most common methods used for contaminant detection. Table 2 compares the general method and the MI sensor system. The sensitivity of a metal detector depends on the conductivity of a metal contaminant. Magnetic metallic contaminants can be easily detected by magnetizing them. X-ray examination can detect a broad range of foreign substances such as stone, glass, bone, resin as well as metal, but cannot be used for dairy products because of the ionization of food or the extinction of good bacteria by the X-rays. To overcome these problems, the SQUID sensing method has a sensitivity higher than pT ( $10^{-12}$  T) and some SQUID detection systems for detecting contaminants in food have been developed<sup>13)–16)</sup>. The maximum velocity of the belt conveyor of a SQUID detection system is about 100 m/min<sup>8)</sup>, but the contaminant detection system using the MI gradiometer is at the design stage and SUS304 balls are moved at 7.5 m/min to correctly measure the magnetic signal of the stainless steel balls. On the other hand, the installation and maintenance costs are higher as SQUID needs a cooling device with liquid helium and



(a) Comparison between value measured with MI gradiometer,  $\Delta B$ , and theoretical value derived from Eq. (3)



(b) Value measured with fluxgate sensor

**Fig. 10** Dependence of variation of magnetic field with movement of SUS304 ball (0.3 mm diameter) and various distances  $r$  between sensor head and steel ball.

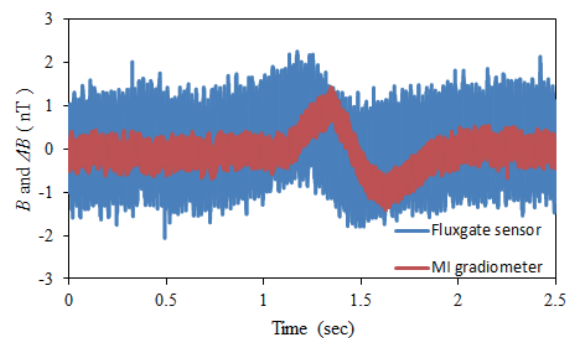


**Fig. 11** Comparison between output of MI gradiometer and fluxgate sensor at  $r = 25$  mm.

magnetic shield system. Since the MI gradiometer can reduce the environmental magnetic noise without the magnetic shield, we consider that the MI sensor is a compact, simple method that can detect small metallic contaminants.

### 5. Conclusions

We developed a first-order gradiometer-type MI sensor (MI gradiometer) and used it to detect SUS304 stainless steel balls.

First, we confirmed that the developed MI gradiometer operated correctly by measuring an artificial signal (amplitude: 2.5 nT, frequency: 10 Hz) with a one-turn coil. The environmental magnetic noise of the MI gradiometer from 1 Hz to 30 Hz was about 20 pT/Hz<sup>1/2</sup>. In particular, noise at 60 Hz relating to the power source line was reduced by at least 1/5 compared with a commercial fluxgate sensor.

Secondly, we measured the variation of the magnetic field with a moving SUS304 ball by using the MI gradiometer and fluxgate sensor. SUS304 balls were magnetized toward the sensor head and were rotated at 7.5 m/min on a turntable. The value measured with the MI gradiometer,  $\Delta B$ , corresponded with the theoretical value calculated by Eq. (3). When we measured a SUS304 ball of 0.3 mm diameter, the lowest detectable magnetic field of each sensor was 1.20 nT (MI gradiometer) and 5.28 nT (Fluxgate sensor).

Since the developed MI gradiometer could detect the magnetic field of SUS304 balls of 0.15 mm, 0.3 mm, 0.5 mm, 0.8 mm, 1.0 mm and 1.5 mm diameters, we consider that the MI sensor can be used in a system for detecting metallic contaminants and that the risk of metal remaining in food can be reduced by using this sensor together with an existing system such as X-ray examination.

**Acknowledgment** The authors sincerely thank Takeshi Kato, an associate professor at Nagoya University, for kindly measuring the residual magnetic moment of SUS304 for this study.

### References

- 1) E. Portalier, B. Dufay, S. Saez, and C. P. Dolabdjian : *10th European Conference on Magnetic Sensors and Actuators (EMSA14)*, (2014).
- 2) L. V. Panina and K. Mohri : *Appl. Phys. Lett.*, **65** (90), 1189–1191 (1994).
- 3) C. M. Cai, Y. Nakamura, K. Mohri, Y. Honkura, and M. Mori : *J. Magn. Soc. Jpn.*, **26** (4), 551–554 (2002).
- 4) S. Godoshnikov, N. Usov, A. Nozdrin, M. Ipatov, A. Zhukov, and V. Zhukova : *Status Solidi A*, DOI 10.1002/pssa.201300717, (2014).
- 5) B. Dufay, S. Saez, C. P. Dolabdjian, A. Yelon, and D. Menard: *IEEE Sensors Journal*, **13** (1), 379–388 (2013).
- 6) B. Dufay, S. Seaz, C. Dolabdjian, A. Yelon, and D. Menard: *IEEE Transactions on Magnetics*, 49 (1), 85–88 (2013).
- 7) Incorporated Administrative Agency National Life Center news release document: “Consultation and summary about the alien substance mixture of the food” (2015).
- 8) S. Tanaka : *Journal of the Japanese Society for Non-Destructive Inspection*, **63** (11), 556–561 (2014).
- 9) T. Uchiyama : *Journal of the Japanese Society for Non-Destructive Inspection*, **63** (11), 562–566 (2014).
- 10) K. Miura, S. Kobayashi, Y. Kamada, Y. Onuki and J.A. Szpunar : *J. Japan Inst. Met. Mater.*, **78** (10), 375–380 (2014).
- 11) K. Ota: “*Jikikugaku no Kiso*”, 25–26 (Kyoritsuzensyo, Tokyo, 1973).
- 12) H. Watabiki, T. Takeda, S. Mitani, T. Yamazaki, M. Inoue, H. Koba, I. Miyazaki, N. Saito, S. Wada, T. Kanai : *Anritsu Technical*, No.87, 53–59 (2012).
- 13) T. Nagaishi, H. Ota, K. Nishi, K. Kuwa, T. Fujita, and S. Tanaka : *IEEE Trans. Appl. Supercond.*, **17** (2), 800–803 (2007).
- 14) S. Tanaka, H. Fujita, Y. Hatsukade, T. Nagaishi, K. Nishi, H. Ota, T. Otani, and S. Suzuki : *Supercond. Sci. Technol.*, **19**, S280-S283 (2006).
- 15) H. J. Krause, G. I. Panaitov, N. Wolter, D. Lomparski, W. Zander, Y. Zhang, E. Oberdoerffer, D. Wollersheim, and W. Wilke : *IEEE Trans. Appl. Supercond.*, **15** (2), 729–732 (2005).
- 16) M. Bick, P. Sullivan, D. L. Tilbrook, J. Du, B. Thorn, R. Binks, C. Sharman, K. E. Leslie, A. Hinsch, K. Macrae, and C. P. Foley : *Supercond. Sci. Technol.*, **18**, 346–351 (2005).

**Received Oct. 20, 2015; Revised Dec. 11, 2015; Accepted Jan. 29, 2016**